JOURNAL OF MATERIALS SCIENCE **34** (1999) 2159–2162

Stress corrosion studies of ion implanted austenitic steel

X. L. ZHANG
Department of Applied Physics, Central South Univ. of Technology, Changsha 410083, People's Republic of China
E-mail: zhang@padova.infm.it

J. C. JIN, Z. XIE
Department of Applied Physics, Hunan University, Changsha 410012, People's Republic of China

J. M. LI
Department of Mechanical Engineering, Hunan University, Changsha 410012, People's Republic of China

P. D. WANG
Institute of semiconductor, Beijing 100080, People's Republic of China

G. B. LIU, B. LONG
Corporation of Dongfang Generator, Deyang 610000, People's Republic of China

Stress corrosion studies of 50 Mn18Cr4 austenitic steel implanted with 120 keV N^+, 100 keV Cr^+, 200 keV and 400 keV Er^+ ions were carried out by constant strain method in the nitrate solution. Surface composition and depth profiles of the implanted material were measured by AES sputter etching technique. The results exhibit that nitrogen implantation has no significant affection to the stress corrosion, but the chromium and erbium implantation has prolonged the incubation period of the stress corrosion cracking.

1. Introduction

The effects of ion implantation on corrosion characteristics for different elements have been studied extensively for a long time [1–3]. It has been reported that N, Cr, Mo, Pt and other ion implantation can improve the corrosion behavior of iron, aluminum, copper and alloys. The improvements of aqueous corrosion resistance have been found due to formation of amorphous or metastable structures [4–7]. Inhibition of surface oxidation due to formed passive layers has also been reported [2]. *However, on stress corrosion, it has not been reported as more as that on general corrosion.*

In this work we have studied the modification induced by N, Cr and Er ion implantation in austenitic steel on the stress corrosion in nitrate solution. The 50 Mn18Cr4 austenitic steel was chosen for present study because it is used for making the generator retaining rings in China and it is susceptible to stress corrosion cracking (SCC) [8]. As doping materials with rare-earth elements *has usually got good effects to improve the toughness* of materials and not affect their strength, it is of special interest to investigate the stress corrosion behavior by doping the high strength austenitic steel with Er.

2. Experimental

2.1. Sample preparation

The used material is taken from a 200 MW generator retaining ring. The composition and the mechanical properties of the 50Mn18Cr4 steel are shown in Table I. The dimensions of the samples were 110 mm × 9.0 mm × 5.0 mm (±0.1 mm) for stress corrosion tests and 10 mm × 9 mm × 1mm for AES analysis. Sample preparation consisted of metallographic polishing with diamond paste down to a grain size of 1/4 μm. After polishing, the specimens were rinsed in ethanol and distilled water. The samples were checked with the ultrasonic wave instruments and there was no observable cracking inside.

2.2. Ion implantation

The ion implantation was carried out with the LC-4 high energy ion implanter at the Institute of Semiconductor in Beijing. The implantation conditions are the following:

Sample A1,
N^+ 120 keV, 2×10^{17} ions/cm^2;

TABLE I Chemical composition and mechanical properties of 50Mn18Cr4 steel

Composition (wt %)	Mn	Cr	C	W	Si	P	S	Fe
	18.0	4.2	0.56	0.58	< 0.52	< 0.05	< 0.01	rest

Mechanical properties	σ_s (MPa)	σ_b (MPa)	δ (%)	Ψ (%)
	902–932	1100–1160	30–48	40–52

Where σ_b means the tensile strength; σ_s, the yield strength; δ, the percentage elongation after fracture on original length and; Ψ, the percentage reduction area of the material.

TABLE II Theoretic ion implantation parameters, projected ranges, R_p; standard deviation in ranges, ΔR_p; and maximum atomic concentration of implantation in 50Mn18Cr4 steel

Ion	Energy (keV)	Dose (ions/cm^2)	R_p (nm)	ΔR_p (nm)	Max. concn. (at %)
N^+	120	2×10^{17}	151	51	1.8
N^+	120	3×10^{17}	151	51	2.8
Cr^+	100	1.5×10^{15}	33	15	0.92
Er^+	400	2×10^{15}	48	17	0.55
Er^+	200	2×10^{15}	27	9.9	0.95

Sample A2,
N^+ 120 keV, 3×10^{17} ions/cm^2;
Samples A3–A7,
Cr^+ 100 keV, 1.5×10^{15} ions/cm^2,
$+ Er^+$ 400 keV, 2×10^{15} ions/cm^2,
$+ Er^+$ 200 keV, 2×10^{15} ions/cm^2,
$+ Cr^+$ 100 keV, 1.5×10^{15} ions/cm^2,
(on the top surface of the samples); and
Cr^+ 100 keV, 1.5×10^{15} ions/cm^2
(on the two sides of the samples).

The calculated ion implantation parameters are reported in Table II. Subsequent implants, of different energies, were performed in order to get a mean distribution of the doping ions in a relatively deep range. The doses were determined with a Faraday cup. The gas pressure in the experimental chamber was about 4×10^{-6} Torr. A liquid nitrogen cool trap was mounted closed to the target holder. The temperature of the target was lower than 100 °C during the process of ion implantation.

2.3. Sample characterization

The stress corrosion behavior was characterized using the constant strain method. The samples were divided in three groups and immersed in two kinds of nitrate solutions. The first kind solution is a mixture of 2% NH_4NO_3 and 26% $Ca(NO_3)_2$ and the second is 3% NH_4NO_3 and 36% $Ca(NO_3)_2$. The temperature of solution was kept at (80 ± 0.5) °C.

The loading device is shown in Fig. 1. The load stress σ is taken as $0.6\,\sigma_s$ and the deflection (Y) of a loaded sample could be calculated from the following formula:

$$Y = (3L^2 - 4C^2)\sigma/12Ed \quad (1)$$

where L is the distance between the two outside support points; C is the distance between inside and outside support points; d is the thickness of the specimen and E is the Young's modulus of the steel. We took $\sigma = 5.5 \times 10^8$ N/m^2; $E = 2 \times 10^{11}$ N/m^2; $d = 5 \times 10^{-5}$ m; $L = 0.1$ m; $C = 0.0375$ m. Then we got $Y = 1.12 \times 10^{-3}$ m.

The magnifying glass is used to check the appearance of the cracking. The length about 0.5 mm is chosen as the mark of the appearance of SCC.

In the cases of Cr and Er implantation, the element depth concentration distributions were measured by sputter etching combined with AES analysis which is carried out with a PHI 550 Scanning Auger Microprobe at the Institute of Semiconductor in Beijing. The cracking morphology was investigated by metallography. The surface composition and state of implanted and non implanted specimens were analyzed by XPS and SIMS. The compositions on grain boundaries were analyzed by Energy-Dispersive X-Ray analyzer. Details of such characterizations will be discussed in a separate work.

3. Result

The measured appearance time of the SCC of the specimens in the mixed nitrate solution is shown in Table III. In the first group, for the samples implanted with N

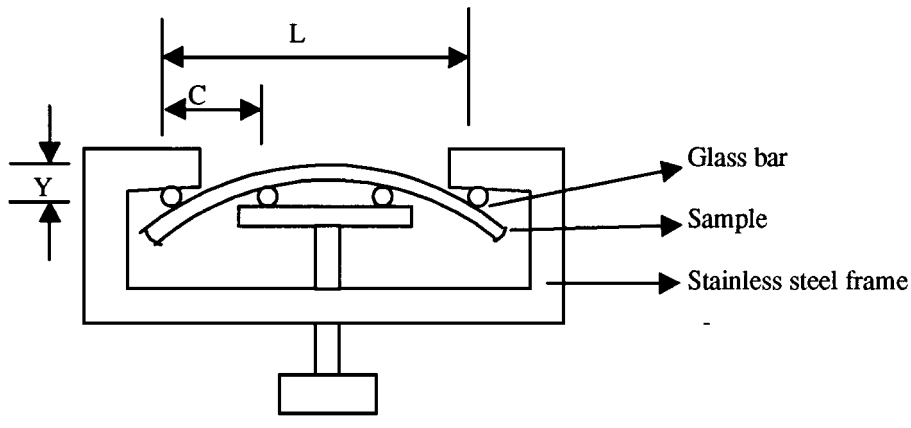

Figure 1 Schematic of the loading device.

TABLE III The results of SCC test with load stress 550 MPa in nitrate solution

Group	Sample		Environment	Incubation time of SCC (h)	
	A1[a]		2% NH_4NO_3	14.9	
1		A2	+		16.0
	B1[b]		26 % $Ca(NO_3)_2$	15.4	
		B2			16.8
	A3			19.7	
	A4		2 % NH_4NO_3	19.0	
2		A5	+		19.0
	B3		26 % $Ca(NO_3)_2$	18.0	
	B4			15.0	
		B5			16.0
	A6		3 % NH_4NO_3	36.2	
3		A7	+		8.8
	B6		36 % $Ca(NO_3)_2$	7.2	
		B7			7.2

[a]Sample A1, A2: implanted with N^+ and A3∼A7 with $Cr^+ + Er^+$.
[b]Sample B1∼B7: unimplanted.

ion (samples A1, A2) and unimplanted, the incubation times have no much significant difference. In the second group, however, the Cr and Er implantation has delayed the appearance of cracking in the nitrate solution. The SCC incubation time of the implanted samples was prolonged averagely as 1.2 times of that of unimplanted one. In the third group, it was prolonged from 1.2 to 5 times.

The cracking morphology of the Cr and Er implanted and unimplanted samples indicated that the stress corrosion cracking in this kind of material in the nitrate solution follows an intergranular path. Compared to the implanted one the unimplanted sample has more, bigger and deeper pits on the surface.

In addition to the corrosion studies, AES depth profiles of Cr and Er implanted and unimplanted samples were carried out. Fig. 2 shows the results of such a depth concentration distribution measurement for a few elements of interest. For the unimplanted sample, the surface signal of oxygen is strong, while for the implanted sample, the strongest surface signal is carbon. This is typical for an implanted metal surface. Oxygen signal has a peak at the time of Ar^+ sputter 8 min for the implanted one, which is caused by ion recoil implantation. Chromium signal has a peak after Ar^+ sputter 15 min. The erbium signal is not strong because the concentration of doped erbium is low. From B. J. Smith's maximum concentration of doped erbium is estimated at 0.95% down to the depth 48 nm, and added chromium at 0.92% down to the depth 63 nm. These values are consistent with that of $d = R_p + 2\Delta R_p$ calculated by Table II. Owing to the subsequent implantation, the Cr and Er atoms implanted were approximately distributed evenly in the sub-layer.

4. Discussion

Generally, the mechanism of the SCC process in ferrous alloy steels in nitrate environment is an anode process involving enhanced and localized anodic dissolution. The accumulation of nitrogen or carbon on the intergrain causes the material corroding as a node in the near area where the concentration of carbon is lower [8].

Many reports indicated that N^+ implantation in iron and alloy steel had improved the material's pitting resistance. Several authors have reported evidence for nitride formation after N^+ implantation in ferrous alloys at ion dose in excess of $2 \times 10^{17}/cm^2$ [4, 9]. Hartley has shown that the process of ion implantation can introduce quite high residual compressive stress into the surface layers of metals [10]. But, in our case, in Table III, it is shown that the samples implanted with N^+ have no significant effect on stress corrosion behavior in the nitrate solution. It suggests that the ion implantation process itself does not affect the stress corrosion resistance of the steel.

The sub-surface layer of iron nitride, which acts as a diffusion barrier in the implanted material, can result in the beneficial pitting characteristics. But under the affection of stress, the micro cracking will emerge on

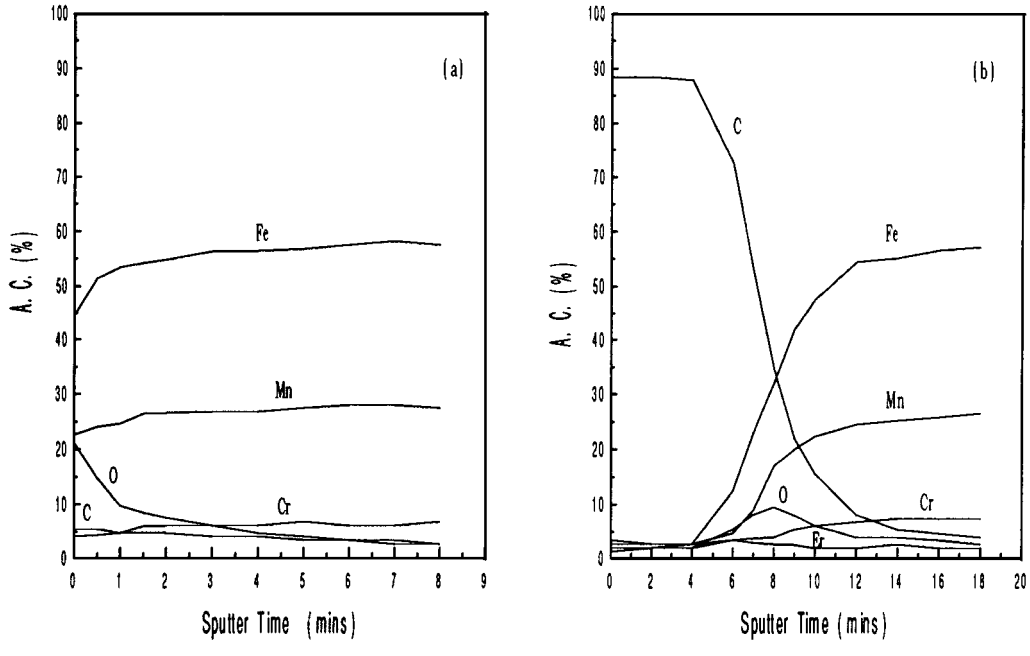

Figure 2 Auger depth profile performed with Ar^+ sputtering for: (a) unimplanted and (b) Cr^+ and Er^+ implanted sample.

the surface due to the existent defects. Hence, N^+ implantation in iron alloys has beneficial effects on pitting resistance, but no effect on stress corrosion.

However, it is interesting to note, with the experimental conditions under which the present work was performed, that a prolonged incubation time for stress corrosion cracking is observed for the samples implanted with chromium and erbium.

Here, it is not clear which mechanism underlying is responsible for the effects. Ashworth has concluded that the effect of the initial contamination was minimal [2]. Thus the beneficial effect of ion implantation on the stress corrosion of 50Mn18Cr4 steel is not due to the presence of cracked hydrocarbons or to the surface damage induced by ion implantation. Rather the effects observed maybe attributed to the chemical nature of ion implanted. Fig. 2 indicates that under the surface there is an abundant oxygen zone. Chromium and erbium are easily combined with oxygen to form Cr_2O_3 and Er_2O_3, which act as a stable passive layer. Thus, enhanced oxidation and the formation of passive layer in nitrate solution probably do play a significant role here.

5. Conclusion

Nitrogen implantation in metals have shown beneficial friction, wear, hardness and pitting characteristics in some cases, but here, it has no significant effect on stress corrosion of 50Mn18Cr4 austenitic steel in nitrate solution. However, the Cr and Er implantation, in this case, has improved the stress corrosion behavior. The incubation time of SCC has been prolonged from 1.2 to 5 times.

It is still an open question under which implantation conditions the most advantageous changes of the corrosion characteristics may be obtained. However, the formation of chromium and erbium oxide layer, acting as a passive film, seems to play an important role in this context.

Acknowledgements

The authors wish to acknowledge the financial support of Foundation for Ion Beam Research Department in the Institute of Metallurgy in Shanghai.

References

1. G. DEARNALEY, J. H. FREEMAN, R. S. NELSON and J. STEPHEN, "Ion Implantation" (Amsterdam, 1973) p. 729.
2. V. ASHWORTH, R. P. PROCTER and W. A. GRANT, in "Treaties on Materials Science and Technology," edited by J. K. Hirvonen (1980) Vol. 18, p. 175.
3. G. K. WOLF, *Surf. Coat. Technology* **83** (1996) 1.
4. M. BRAUN, S. HULTBERG, A. BROWN, B. M. SVENSSON and S. HOGMARK, *Nucl. Instrum. and Meth. B.* **19/20** (1987) 259.
5. A. G. DUFFY, L. CLAPHAM, J. L. WHITTON and M. C. RIDGWAY, *ibid.* **106** (1995) 504.
6. K. C. WALTER, R. A. DODD and J. R. CONRAD, *ibid.* **106** (1995) 522.
7. S. Y. WANG, P. K. CHU, B. Y. TANG, X. C. ZENG and X. F. WANG, *ibid.* **127/128** (1997) 1000.
8. J. C. JIN, J. M. LI, Z. XIE, X. L. ZHANG, P. D. WANG, G. B. LIU and B. LONG, *J. Hunan Univ.* **19** (1) (1992) 1.
9. S. FAYEULLEAND and D. TREHEUX, *Nucl. Instrum. and Meth. B* **7/8** (1985) 171.
10. N. E. W. HARTLEY, *J. Vac. Sci. Technol.* **12** (1975) 485.

Received 26 February
and accepted 26 October 1998